ELSEVIER

PII: S0032-3861(97)10270-1

Polymer Vol. 39 No. 15, pp. 3473–3477, 1998

0032-3861/98/$19.00+0.00

Phase behaviours of solid polymer electrolytes: applicability of the melting point depression

Jung Yong Kim[a], Si-Tae Noh[b] and Young Chan Bae[a,*]
[a]*Department of Industrial Chemistry and Molecular Thermodynamics Laboratory, Hanyang University, Seoul 133-791, South Korea*
[b]*Department of Chemical Engineering, Hanyang University, Ansan, 435-791, South Korea*
(Accepted 7 November 1997)

Thermal analysis of poly(ethylene oxide) (PEO) with three different salts, $MnBr_2$, MnI_2 and $LiCF_3SO_3$ has been carried out at various temperatures and compositions. Optical microscopy and differential scanning calorimetry have been used to collect data necessary for the phase diagrams. The melting point depression phenomena are observed to be explicable in terms of thermodynamic equilibrium of the amorphous phase with the crystalline phase. To this end, a thermodynamic model appropriate to describe the crystalline–amorphous phase in the semicrystalline polymer is developed based on an extended Flory–Huggins equation. Quantitative description according to the proposed model is in good agreement with the experimentally observed transition temperature of a given system including an eutectic point. © 1998 Elsevier Science Ltd. All rights reserved.

(Keywords: melting point depression; extended Flory–Huggins equation; eutectic point)

INTRODUCTION

Since Fenton *et al.*[1] and Armand *et al.*[2] showed that solid polymer electrolytes (SPE) consisting of poly(ethylene oxide) (PEO) and an alkali metal salt have significant ionic conductivities and can be used in all solid-state electrochemical batteries, considerable research has been directed toward the development of polymer electrolytes having high ionic conductivity at room temperature. The objective has been to identify solid polymer electrolytes with a conductivity higher than 10^{-3} S cm^{-1}, and a redox stability window higher than 4 V, which is the lower limit in the case of utilisation of high-voltage cathodes. To approach the above-mentioned properties of SPE for batteries application, the polymer should have both low T_g and low crystallinity, and the salt ought to have a large anion delocalised of the negative charge to reduce ion–ion interactions and be ionised in polymer (solid solvent), not only to build up charge carriers but also to increase the crystallinity in the polymer matrix by interaction between base group (e.g. oxygen in PEO) of polymer and cation from salt. As a result, there is an optimum condition for this competition between the build-up of charge carrier and the consequential increase in T_g for SPE to be applied to battery materials[3].

There are two broad classes of SPE; the first consists of solvent-free, conventional polymer electrolytes comprising a high molecular weight polymer host and a Li salt; the second group consists of electrolytes which contain, in addition to the polymer host and Li salt, a significant proportion of liquid solvents, termed plasticisers[4].

In this study, we limited our discussion to solvent-free electrolytes and to the choice of a thermodynamic approach that makes it possible to interpret phase behaviours of polymer/salt systems.

* To whom correspondence should be addressed

Smith and Pennings[5] showed that, according to the Flory–Huggins theory of melting point depression, a eutectic point may occur in an athermal polymer/diluent system if melting point of the diluent is not too low in comparison with that of the polymer. Gryte *et al.*[6] reported that crystallisation characteristics of the PEO/glutaric acid binary system were determined. Myasnikova *et al.*[7] provided the phase diagram of the PEO/resorcinol system, in which resorcinol molecules form hydrogen bonds to the polymer chain. Wittmann and co-workers[8] presented the crystallisation and the crystalline morphology of the binary system, polyethylene/1,3,5-tribromobenzene, which again displays both eutectic solidification and oriented growth of the polymer crystals.

A similar approach has been also applied to the study of SPE. Stainer *et al.*[9] constructed a phase diagram for the PEO/NH_4SCN system. Lee and Crist[10] reported the phase behaviour of PEO/NaSCN mixtures which form a eutectic reaction. Fauteux and co-workers[11–14] extensively studied phase behaviours of binary SPE systems such as PEO/LiX ($X = CF_3SO_3^-$, ClO_4^-, AsF_6^-, $N(CF_3SO_2)_2^-$, $C(CF_3SO_3)_3^-$) and PEO/NaI.

However, in previous studies of the phase behaviour of SPE, it is hard to find a theoretical prediction which can describe and predict liquidus curves including a eutectic point. In this study, we modified an extended Flory–Huggins equation[15,17] based on Flory's melting point depression concept and compared our calculated model with experimental data (melting points) of PEO/$LiCF_3SO_3$[11,20–23], PEO/MnI_2, PEO/$MnBr_2$ and polyethylene (PE)/1,3,5-tribromobenzene[8] systems.

THEORY

Two theoretical aspects are taken into account; one is the modification of an extended Flory–Huggins equation; the

other is Flory's melting point depression of polymers which well describes the effect of diluents, copolymerised units, and end groups on the melting point when the concentration of each is low[16].

When we consider a salt effect of the free energy of mixing, we assume that the salt is a particle, and the consequential decrease of entropy should be corrected in the interaction energy term (χ).

Correlating equations

For a binary polymer/salt system, the Flory–Huggins expression for the molar Gibbs energy of mixing ΔG at a temperature T is given by[16]

$$\frac{\Delta G}{RT} = \frac{\phi_1}{r_1}\ln\phi_1 + \frac{\phi_2}{r_2}\ln\phi_2 + \chi_{FH}\phi_1\phi_2 \quad (1)$$

where R is the gas constant; ϕ_1, ϕ_2, r_1, and r_2 are volume fractions and relative molar volumes of components 1 and 2, respectively, and χ_{FH} is the Flory–Huggins interaction parameter. Recently, Qian *et al.*[17,18] suggested a semiempirical form for χ. They replaced χ_{FH} by $g(T,\phi_2)$, a function of temperature and concentration. The Gibbs free energy of mixing and chemical potentials in terms of the new interaction parameter χ from the relation, $\chi = g - \phi_1 g'$, are given by

$$\frac{\Delta G}{RT} = \frac{1-\phi_2}{r_1}\ln(1-\phi_2) + \frac{\phi_2}{r_2}\ln\phi_2 + \phi_2\int_{\phi_2}^{1}\chi(T,\phi)\,d\phi \quad (2)$$

$$\frac{\Delta\mu_1}{RT} = \ln(1-\phi_2) + \phi_2\left(1-\frac{r_1}{r_2}\right) + \chi(T,\phi_2)r_1\phi_2^2 \quad (3)$$

$$\frac{\Delta\mu_2}{RT} = \ln\phi_2 + (1-\phi_2)\left(1-\frac{r_2}{r_1}\right) - r_2\phi_1\phi_2\chi(T,\phi_2) + r_2\int_{\phi_2}^{1}\chi(T,\phi)\,d\phi \quad (4)$$

Qian *et al.*[19] proposed that χ is given by the product of a temperature-dependent term, $D(T)$, and a concentration-dependent term, $B(\phi)$:

$$\chi(T,\phi) = D(T)B(\phi_2) \quad (5)$$

Following Flory[16], Qian *et al.*[17,18] suggest

$$D(T) = d_0 + \frac{d_1}{T} + d_2\ln T \quad (6)$$

where d_0, d_1, and d_2 are constants for a given binary system. For the concentration-dependent term, they use

$$B(\phi_2) = 1 + b_1\phi_2 + b_2\phi_2^2 \quad (7)$$

where b_1 and b_2 are constants for a given binary system.

In this study, we use simple functions of temperature and composition as follows:

$$D(T) = d_0 + \frac{d_1}{T} \quad (8)$$

$$B(\phi_2) = 1 + b\phi_2 \quad (9)$$

where d_0, d_1, and b are adjustable model parameters.

Theory of the melting point depression

In a semicrystalline system, the condition of equilibrium between a crystalline polymer and the polymer unit in the solution may be described as follows[16]:

$$\mu_u^c - \mu_u^0 = \mu_u - \mu_u^0 \quad (10)$$

where μ_u^c, μ_u, and μ_u^0 are chemical potentials of crystalline polymer segment unit, of liquid (amorphous) polymer segment unit and chemical potential in standard state, respectively. Now the formal difference of appearing on the left-hand side is expressed as follows:

$$\mu_u^c - \mu_u^0 = -\Delta H_u(1 - T/T_m^0) \quad (11)$$

where ΔH_u is the heat of fusion per segment unit, T and T_m^0 are melting temperature of the species in a mixture and of the pure phases, respectively. The right-hand side of equation (10) can be restated as follows:

$$\mu_u - \mu_u^0 = RT\frac{V_u}{V_1}\left[\frac{r_1}{r_2}\ln\phi_2 + (1-\phi_2)\left(\frac{r_1}{r_2}-1\right) - r_1\phi_1\phi_2\left(d_0 + \frac{d_1}{T_{m,2}}\right)(1+b\phi_2) + r_1\left(d_0+\frac{d_1}{T_{m,2}}\right)\left(1+\frac{b}{2}-\phi_2-\frac{b}{2}\phi_2^2\right)\right] \quad (12)$$

where V_1 and V_u are the molar volumes of the salt and of the repeating unit, respectively.

By substituting equation (11) and equation (12) into equation (10) and replacing T by $T_{m,2}$, the equilibrium melting temperature of mixture is given by

$$\frac{1}{T_{m,2}} - \frac{1}{T_{m,2}^o} = -\frac{R}{\Delta H_u}\frac{V_u}{V_1}\left[\frac{r_1}{r_2}\ln\phi_2 + (1-\phi_2)\left(\frac{r_1}{r_2}-1\right) - r_1\phi_1\phi_2\left(d_0+\frac{d_1}{T_{m,2}}\right)(1+b\phi_2) + r_1\left(d_0+\frac{d_1}{T_{m,2}}\right)\left(1+\frac{b}{2}-\phi_2-\frac{b}{2}\phi_2^2\right)\right] \quad (13)$$

The subscripts 1, 2 and u refer to the salt, the polymer, and polymer segment unit, respectively. Similarly, we obtain

$$\frac{1}{T_{m,1}} - \frac{1}{T_{m,1}^o} = -\frac{R}{\Delta H_1}\left[\ln(1-\phi_2) + \phi_2\left(1-\frac{r_1}{r_2}\right) + \left(d_0+\frac{d_1}{T_{m,1}}\right)(1+b\phi_2)r_1\phi_2^2\right] \quad (14)$$

From equation (13) and equation (14), we can predict liquidus curves in phase diagram of binary polymer/salt systems.

EXPERIMENTAL

Sample preparation

Poly(ethylene oxide) (M_w = 900 000) was obtained from Aldrich Chemical Co. and was used without further purification. Manganese(II) bromide (98%), manganese(II) iodide (99%), lithium-trifluoromethane-sulfonate (96%), and acetonitrile (99.9%) were also supplied by Aldrich Chemical Co. and were used as received. *N,N*-Dimethylformamide (DMF) (reagent grade) was supplied by Tedia company.

For PEO/$MnBr_2$ and PEO/MnI_2 systems, samples were cast in mixed solvents. PEO is dissolved easily in acetonitrile and the salt is dissolved in *N,N*-dimethylformamide (DMF). To form films, known amounts of PEO were dissolved in acetonitrile and manganese halide was dissolved in minimum amounts of DMF. Acetonitrile solution was mixed with DMF solution. The mixture of various O/Mn mole ratios was stirred

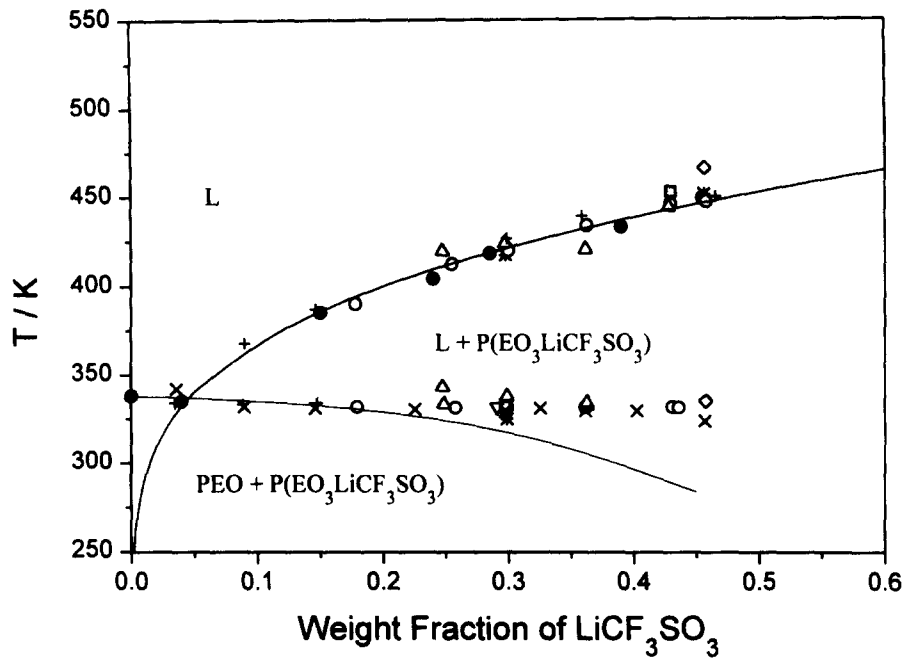

Figure 1 Phase diagram of the PEO/$LiCF_3SO_3$ system. The transition temperatures were obtained using various experimental techniques: n.m.r. ($*^{20}$), DTA or d.s.c. (O^{20}, Δ^{21}, $\diamond^{22}$), conductivity ($\times$ [11], ∇^{20}, $\blacktriangle^{21}$) and optical microscopy (+ [11], $\blacksquare^{23}$). This study: thermo-optical analysis technique (●), theory (sold lines)

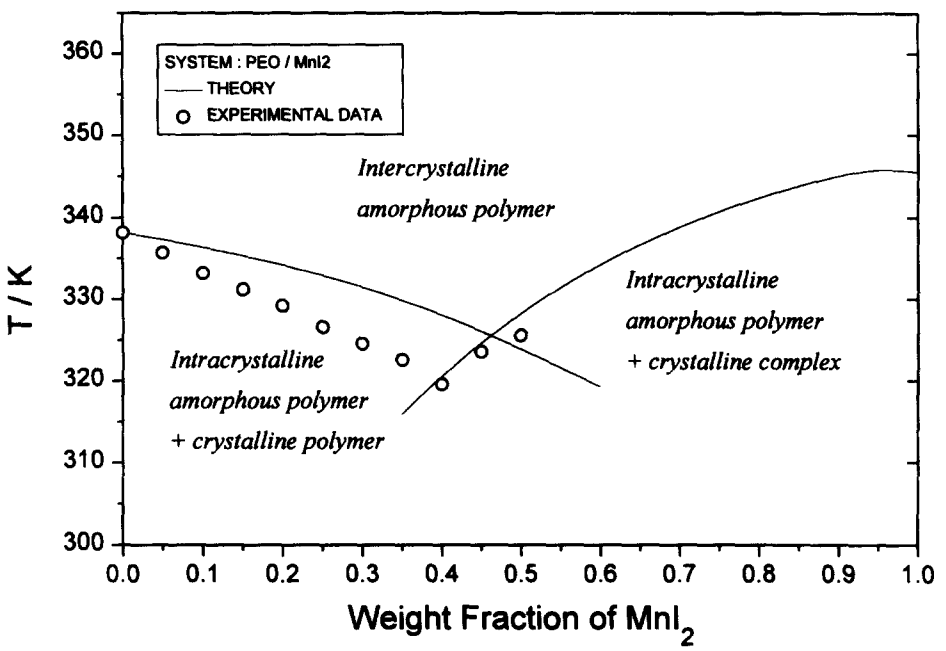

Figure 2 Phase diagram of the PEO/MnI_2 system. The transition temperatures were obtained using a thermo-optical analysis technique, (○). Solid lines are calculated from the proposed model based on an extended Flory–Huggins equation

for 48 h at room temperature, and then cast on a precleaned microscope slide (25 × 75 × 1 mm). Films were air-dried for several hours and then transferred to a vacuum oven. They were dried under vacuum at 90° for 24 h and were not used until crystallisation was completed.

For the PEO/$LiCF_3SO_3$ system, the same procedure described above were used. The difference being that acetonitrile is only used as a solvent.

Thermo-optical analysis

Melting point measurements of polymer electrolyte/salt systems were carried out by thermo-optical analysis (TOA) technique. It consists of a heating–cooling stage, a photodiode (Mettler FP80) and a microprocessor (Mettler FP90). The scan rate was 2.0°C min^{-1}. An IBM PC was used for data acquisition.

Differential scanning calorimetry

A Perkin-Elmer DSC-7 was used to measure the heat of fusion and melting temperature of pure salts at a heating rate of 10°C min^{-1}. The heat of fusion of $MnBr_2$ (T_m^0 = 54.86°C), MnI_2 (T_m^0 = 72.38°C) and $LiCF_3SO_3$ (T_m^0 = 226.14°C) are 2.72, 4.66, and 67.13 J g^{-1}, respectively.

RESULTS AND DISCUSSION

Figure 1 shows phase behaviours of the PEO/$LiCF_3SO_3$ system. Dark circles were measured by TOA and solid lines

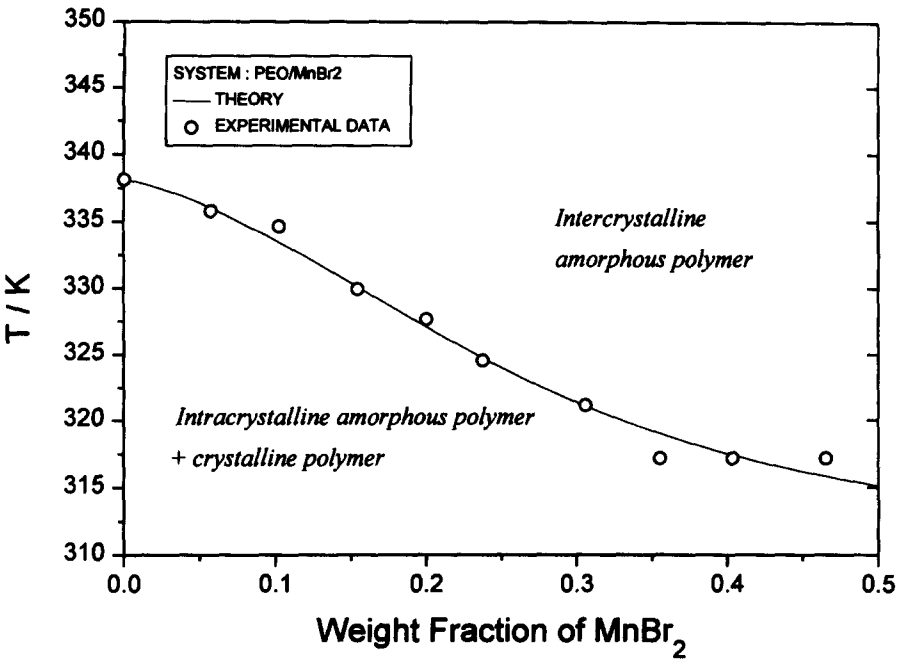

Figure 3 Phase diagram of the PEO/$MnBr_2$ system. The transition temperatures were obtained using a thermo-optical analysis technique (O). The solid line is calculated from the proposed model based on an extended Flory–Huggins equation

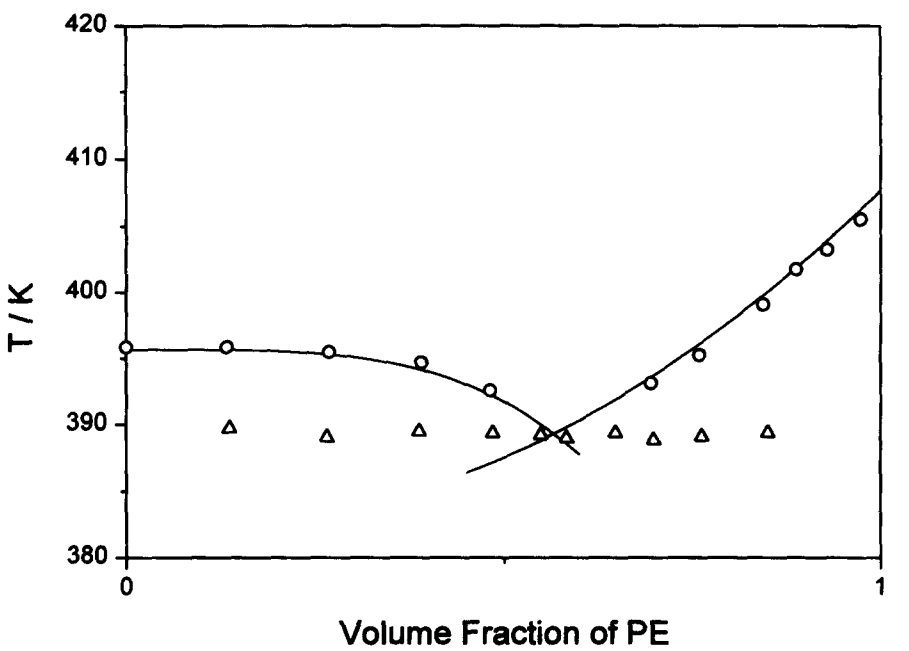

Figure 4 Phase diagram of the PE/1,3,5-tribromobenzene system. The transition temperature was obtained using d.s.c. (O, Δ)[8]. This study: solid lines are calculated from the proposed model based on an extended Flory–Huggins equation

were calculated from the proposed model. Other experimental data were obtained by n.m.r. (*[20]), DTA or d.s.c. (O[20], Δ[21], ◇[22]), conductivity (× [11], ▽[20], ▲[21]) and optical microscopy (+ [11], ■[23]). The melting points obtained by TOA are consistent with data measured by others[11,20–23]. From the proposed model which describes the thermodynamic equilibrium of the amorphous phase with the crystalline phase, equation (13) was used for the calculation of the polymer-rich liquidus curve, and equation (14) for the calculation of the salt-rich one. The density of PEO was taken as 1.21 g cm^{-3}. The density of the $LiCF_3SO_3$ used was 2.69 g cm^{-3}, which was calculated by the group contribution method[24]. By substituting values of R = 1.98 cal K^{-1} mol^{-1}, ΔH_l = 2513.5 cal mol^{-1}, $r_1 = 1$, r_2 = 2594.92, and $T^0_{m,l}$ = 499.29 K into equation (14), the best fit to the salt-rich liquidus curve (solid line on the right-hand side of *Figure 1*) was obtained. Adjustable model parameters are $d_0 = -4.523$, $d_1 = 2304.7$, and $b = -0.253$. Substituting the same adjustable model parameters, ΔH_u = 1980 cal mol^{-1}, V_u = 36.6 cm^3 mol^{-1}, V_l = 52.66 cm^3 mol^{-1} and $T^0_{m,2}$ = 338.15 K into equation (13) gives the solid line on the left-hand side of *Figure 1*. As shown in *Figure 1*, the theoretical prediction not only gives an excellent agreement with experimental results but also identifies the eutectic point at the intersection of the two liquidus curves at a weight fraction of $LiCF_3SO_3 \approx 0.05$.

Figure 2 shows the phase behaviour of the PEO/MnI_2 system. Open circles were obtained by TOA and solid lines were calculated from the proposed model. It was observed that no crystalline complex is formed below a weight

Table 1 Melting temperature, heat of fusion, molecular weight, density, and molar volume for each sample

	T_m^0 (K)	ΔH (cal mol^{-1})	M_w (g mol^{-1})	Density (g cm^{-3})	V (cm^3 mol^{-1})
PEO	338.15	1980	900 000	1.21	36.6
PE	395.65	980	Marlex50	0.80	14.6
$LiCF_3SO_3$	499.29	2513.5	156.01	2.69	52.66
MnI_2	345.53	345.3	308.75	5	61.75
$MnBr_2$	328.32	140.2	214.76	4.385	48.98
1,3,5-Tribromo-benzene	407.65	690	314.80	2.5	125.9

Table 2 Adjustable model parameters for given systems

	PEO/$LiCF_3SO_3$	PEO/MnI_2	PEO/$MnBr_2$	PE/1,3,5-tribromobenzene
d_0	-0.453×10^1	-0.618×10^2	-0.980×10^3	-0.545×10^0
d_1	0.230×10^4	0.216×10^5	0.310×10^6	0.439×10^3
b	-0.253×10^0	-0.864×10^0	-0.362×10^0	-0.197×10^0

fraction of $MnI_2 \approx 0.4$. Therefore, only normal PEO crystals are present within conventional spherulites up to the eutectic point, and the added salt should reside in the amorphous regions between lamellar crystals. Near the eutectic point (weight fraction of $MnI_2 \approx 0.4$), the transition took place slowly. The dependence of the melting point on the MnI_2 content reveals information about the enthalpy of the interaction between the polymer and the salt. The calculated curves, which have some deviation from experimental results, can be obtained by substituting the values from *Table 1–Table 2* into equations (13) and (14).

Figure 3 shows the phase behaviours of the PEO/$MnBr_2$ system. Open circles were obtained by TOA and the solid line was calculated from the proposed model. The transition temperature decreases with increasing weight fraction of $MnBr_2$ and then levels off around a weight fraction of $MnBr_2 \approx 0.35$. Our experimental results show that the system is partially crystalline at room temperature. Theoretical prediction can be obtained by substituting the values from *Tables 1 and 2* into equation (13). However, we could not observe a salt-rich liquidus curve which is known to vary considerably with the crystallisation conditions. As shown in *Figure 3*, a good agreement is attained between calculated polymer-rich liquidus curve and the observed melting point depression.

Figure 4 shows a phase diagram of the PE/1,3,5-tribromobenzene system, which is a non-electrolyte system reported by Hodge *et al.*[8]. Open circles and upright triangles were measured by d.s.c.[8]. In this study, taking the estimated adjustable model parameters (*Table 2*) and the same physical data (*Table 1*) that Hodge *et al.* reported in their paper, we calculated liquidus curves (solid lines). Our theoretical model predicts very well the phase behaviour and the eutectic point for a given system.

CONCLUSIONS

A polymer-based binary system is subject to the laws of classical thermodynamics and can be described by phase diagrams. As a result of thermal analysis, the phase diagrams were constructed and the liquidus curves between a crystalline phase and an amorphous phase were calculated from an extended Flory–Huggins equation based on Flory's melting point depression concept. The proposed model describes very well phase behaviours not only of a polymer/diluent system (PE/1,3,5-tribromobenzene) but also of polymer/salt systems (PEO/$LiCF_3SO_3$, PEO/MnI_2 and PEO/$MnBr_2$). It also predicts remarkably well a eutectic point at the intersection of two liquidus curves for a given system.

ACKNOWLEDGEMENTS

This paper was supported by Research Fund (9606-060), Korea Research Foundation (December, 1996).

REFERENCES

1. Fenton, B.E., Parker, J.M. and Wright, P.V., *Polymer*, 1973, **14**, 589.
2. Armand, M., Chabagno, J. M. and Duclot, M., in: *Fast Ion Transport in Solids*, ed. P. Vashishta, J. N. Mundy and G. K. Shenoy. North-Holland, Amsterdam 1979, p. 131.
3. Cowie, J.M.G. and Martin, A.C.S., *Polymer*, 1987, **28**, 627.
4. Alamgir, M. and Abraham, K. M., in: *Lithium Batteries New Materials, Developments and Perspectives*, Vol. 5, ed. G. Pistoia. Elsevier, 1994, p. 93.
5. Smith, P. and Pennings, A.J., *J. Polym. Sci.*, 1977, **15**, 523.
6. Gryte, C.C., Berghmans, H. and Smets, G., *J. Polym. Sci.*, 1979, **17**, 1295.
7. Myasnikova, R.M., Titova, E.F. and Obolonkova, E.S., *Polymer*, 1980, **21**, 403.
8. Hodge, A.M., Kiss, G., Lotz, B. and Wittmann, J.C., *Polymer*, 1982, **23**, 985.
9. Stainer, M., Hardy, L.C., Whitmore, D.H. and Shriver, D.F., *J. Electrochem. Soc.*, 1984, **131**(4), 784.
10. Lee, Y.L. and Crist, B., *J. Appl. Phys.*, 1986, **60**(8), 2683.
11. Robitaille, C.D. and Fauteux, D., *J. Electrochem. Soc.*, 1986, **133**(2), 315.
12. Fauteux, D., *J. Electrochem. Soc.*, 1987, **134**(11), 2761.
13. Fauteux, D., in: *Polymer Electrolyte Reviews—1*, ed. J. R. MacCallum, and C. A. Vincent. Elsevier, 1987, p. 121.
14. Fauteux, D. and McCabe, P., *Polym. Advanced Technol.*, 1995, **6**, 83.
15. Bae, Y.C., Shim, J.J., Soane, D. S. and Prausnitz, J.M., *J. Appl. Polym. Sci.*, 1993, **47**, 1193.
16. Flory, P. J., in: *Principles of Polymer Chemistry*. Cornell University Press, Ithaca, NY, 1953.
17. Qian, C., Munby, S.J. and Eichnger, B.E., *Macromolecules*, 1991, **24**, 1655.
18. Qian, C., Munby, S.J. and Eichnger, B.E., *J. Polym. Sci. Part B*, 1991, **29**, 635.
19. Barton, A. F., in: *Handbook of Solubility Parameters and Other Cohesion Parameters*. CRC Press, Boca Raton, FL, 1983.
20. Minier, M., Berthier, C. and Gorecki, W., *J. Phys.*, 1984, **45**, 739.
21. Weston, J.E. and Steele, B.C.H., *Solid State Ionics*, 1981, **2**, 347.
22. Payne, D.R. and Right, P.V., *Polymer*, 1982, **23**, 690.
23. Papke, B.L., Ratner, M.A. and Shriver, D.F., *Polymer*, 1982, **129**, 1434.
24. Van Krevelen, D. W., in: *Properties of Polymer*. Elsevier, 1990, p. 87.